British Journal of Pharmacology

DOI:10.1111/j.1476-5381.2011.01784.x
www.brjpharmacol.org

RESEARCH PAPER

Dronedarone prevents microcirculatory abnormalities in the left ventricle during atrial tachypacing in pigs

A Bukowska[1], M Hammwöhner[2], A Sixdorf[1], L Schild[3], I Wiswedel[3], F-W Röhl[4], C Wolke[5], U Lendeckel[5], C Aderkast[5], S Bochmann[5], RK Chilukoti[6], J Mostertz[6], P Bramlage[7] and A Goette[1,2]

[1]*Medical Faculty, Otto von Guericke University, Magdeburg, Germany,* [2]*St. Vincenz-Hospital, Paderborn, Germany,* [3]*Institute of Clinical Chemistry, Department of Pathobiochemistry, Medical Faculty, Otto-von-Guericke University, Magdeburg, Germany,* [4]*Institute of Biometrics, Otto-von-Guericke University, Magdeburg, Germany,* [5]*Department of Medical Biochemistry and Molecular Biology, University of Greifswald, Germany,* [6]*Interfaculty Institute for Genetics and Functional Genomics, Department of Functional Genomics, University of Greifswald, Germany, and* [7]*Institute for Pharmacology and preventive Medicine, Mahlow, Germany*

Correspondence
Professor Dr Andreas Goette, St. Vincenz-Hospital, Medical Clinic II, Am Busdorf 2, 33098 Paderborn, Germany. E-mail: andreas.goette@vincenz.de

Keywords
dronedarone; atrial fibrillation; microcirculation; acute coronary syndrome

Received
15 December 2010
Revised
2 November 2011
Accepted
9 November 2011

BACKGROUND AND PURPOSE

Atrial fibrillation induces ischaemic microcirculatory flow abnormalities in the ventricle, contributing to the risk for acute coronary syndromes. We evaluated the effect of dronedarone on ventricular perfusion during rapid atrial pacing (RAP).

EXPERIMENTAL APPROACH

Coronary and fractional flow reserve (CFR/FFR) were measured in the left anterior descending artery in 29 pigs. Six received RAP, six received RAP with dronedarone (RAP/D), seven received dronedarone alone, four received RAP with amiodarone (RAP/A), and six received neither (sham). In ventricular tissue, oxidative stress/ischaemia-related gene and protein expression was evaluated by RT-PCR and Western blotting; Isoprostanes were measured by GC-MS procedures.

KEY RESULTS

CFR was decreased in the RAP group, compared with other groups. FFR was not different between groups. Effective refractory period was reduced in RAP compared with RAP/D. RAP-activated PKC phosphorylation tended to be decreased by dronedarone ($P = 0.055$) RAP induced NOX-1 and NOX-2 protein and the mRNA for hypoxia-inducible factor-1α (HIF-1α). Dronedarone reduced the pacing-dependent increase in the expression of NOX-2 protein and of HIF-1α mRNA. The oxidative stress marker, F_2-isoprostane, was increased by RAP and this increase was attenuated by dronedarone. Other oxidative stress/ischaemia-related genes were induced by RAP compared with sham and were decreased by dronedarone treatment. In HL1 cells, dronedarone significantly inhibited the increased phosphorylation of PKCα after oxidative stress, with an almost significant effect ($P = 0.059$) on that after RAP.

CONCLUSIONS AND IMPLICATIONS

Dronedarone abolished RAP-induced ventricular microcirculatory abnormalities by decreasing oxidative stress/ischaemia-related gene and protein expression in the ventricle.

Abbreviations

ACS, acute coronary syndromes; AF, atrial fibrillation; ATHENA, Prevention of Cardiovascular Hospitalization or Death From Any Cause in Patients with Atrial Fibrillation/Atrial Flutter; CFR, coronary flow reserve; FFR, fractional flow reserve; HIF1α, hypoxia-inducible factor-1α; HR, hazard ratio; LAD, left anterior descending; NOX, NADPH oxidase subunits 1, 2 and 4; PPARGC1, PPARγ coactivator 1-α; PRKAG2, PKA subunit γ-2; RAP, rapid atrial pacing; ROS, reactive oxygen species

Introduction

Patients diagnosed with atrial fibrillation (AF) are at high risk for subsequent coronary ischaemic events (Miyasaka *et al.*, 2007). Recently, the Prevention of cardiovascular hospitalization or death from any cause in patients with atrial fibrillation/atrial flutter ATHENA clinical trial has shown that the incidence of hospitalizations for acute coronary syndromes (ACS) was reduced in patients with AF [hazard ratio (HR) 0.70; 95% confidence interval (CI) 0.51–0.97] when treated with dronedarone, including rate control and anticoagulation (Hohnloser *et al.*, 2009). A subgroup analysis demonstrated that the incidence of ACS was also reduced in patients with coronary artery disease at baseline (HR 0.67; 95% CI 0.46–0.99) (Crijns *et al.*, 2009). The underlying mechanism is, however, largely unknown.

Coronary flow reserve (CFR) is reduced in patients with AF (Saito *et al.*, 1978; Wichmann *et al.*, 1983). This was also described in an *in vivo* rapid atrial pacing (RAP) model where CRF was reduced while fractional flow reserve (FFR) was unaffected (Goette *et al.*, 2009). The major underlying mechanisms appear to be oxidative stress and calcium overload (Goette *et al.*, 2009). The potential of benzofuran derivatives such as dronedarone (or amiodarone) to improve coronary flow has been described previously (Raddino *et al.*, 1989; Guiraudou *et al.*, 2004). Furthermore, there is potential for an interaction of amiodarone and dronedarone with α-adrenoceptors leading to a reduction of coronary vasoconstriction mediated by these receptors (Ertl *et al.*, 1986; Heusch *et al.*, 2000; receptor nomenclature follows Alexander *et al.*, 2011). This has shown to be more pronounced with dronedarone than with amiodarone (Raddino *et al.*, 1989; Hodeige *et al.*, 1995). Guiraudou *et al.*, (2004) further noted that the improvement of coronary flow was dependent on NO, although the dose-dependent effect of dronedarone on NO (0.01–1 μM) differed from that of amiodarone (0.01–10 μM) by a relaxant effect, persisting after inhibition of the NO synthase pathway. A recent study, in a porcine model of myocardial infarction/reperfusion, demonstrated direct cardioprotective activity of dronedarone that was independent of the remaining subendocardial blood flow during ischaemia (Skyschally and Heusch, 2011). Nevertheless, vasoreactive, NO-independent, mechanisms of dronedarone have not been fully elucidated so far.

In order to investigate the potential of dronedarone to reduce oxidative stress-related microvascular abnormalities as well as to elucidate the cellular mechanisms responsible for this effect, we used a relatively short-term exposure (6h) to RAP in pigs as the standard experimental system, together with studies in a cardiomyocyte cell line (HL-1 cells).

Methods

RAP model

All animal care and experimental procedures were approved by the Institutional Animal Care and Use Committee of the University of Magdeburg. A total of 29 pre-medicated, intubated and instrumented pigs (mean weight 30 kg) were randomly assigned to study groups (Goette *et al.*, 2008; 2009). The premedication consisted of i.m. injections of 0.2 ml kg^{-1} ketamine (10% ketamine (Ursotamin®), Serumwerk Bernburg, Germany) and 0.1 ml kg^{-1} xylazine (2% xylazine hydrochloride, (Xylazin®), Riemser Arzneimittel GmbH, Germany). Anaesthesia was induced with 6-10 ml propofol (i.v.; Recofol® 1%, Curamed Pharma GmbH, Karlsruhe, Germany) and maintained with with 1-2 vol% isoflurane (Isofluran Curamed, Curamed Pharma GmbH) in a mixture of O_2 :N_2O (30:70 vol%) via endotracheal tube. Oxygen saturation and ECG were monitored continuously throughout the procedure. RAP was performed in six animals at a rate of 600 beats per minute (twice diastolic threshold, 2 ms pulse duration) for 6 h (RAP group). In further six animals, RAP was performed after treatment with 10 mg·kg^{-1} dronedarone (Sanofi-Aventis, Paris, France; RAP/D group), seven pigs received 10 mg·kg^{-1} dronedarone only (D group), in four pigs, RAP was performed in the presence of 10 mg·kg^{-1} amiodarone (Cordarex®, Sanofi-Aventis, Frankfurt am Main, Germany; RAP/A group) and six pigs were instrumented without any further intervention (sham group). After 6 h of RAP, the chest and the pericardial sac were opened and the heart was exposed. Parts of the anterior wall of the left ventricle were cross-clamped, excised and immediately frozen in liquid nitrogen. The experiments were done in a repetitive order with each sham followed by one animal from the RAP, RAP/D, RAP/A and dronedarone groups, respectively. No animal was excluded from the study. Molecular analyses with regard to protein expression and determination of plasma levels of cardiac markers were done by investigators blinded to the *in vivo* results.

Measurement of CFR and FFR

CFR measurements were performed using a pressure temperature sensor-tipped guide wire (Radi Medical System, Langenhagen, Germany), which also allows the simultaneous determination of the FFR. The CFR measurements are influenced by flow abnormalities in the epicardial arteries and the microcirculation. In contrast, reduced FFR is specific to epicardial lesions. Thus, a normal FFR (non-obstructed epicardial vessels) in the presence of reduced CFR is indicative of microvascular disease (Kern *et al.*, 2006; Camici and Crea, 2007). However, absolute coronary flow was not determined with the system used.

Angiography of the left coronary artery was performed using a 6F guiding catheter. Thereafter, a coronary pressure wire (Radi Medical System) was advanced into the distal left anterior descending (LAD) artery. CFR was calculated using the Radi Medical System software package. In brief, the software allows the pressure sensor, located 3 cm from the tip of the pressure wire, to act also as a distal temperature sensor, whereas the shaft of the wire acts as a proximal temperature sensor. Thus, the transit time of an injectant can be calculated. Saline (3mL at room temperature) was injected into the LAD artery three times. The mean transit time was recorded after each injection and then averaged. Hyperaemia was induced by systemic application of adenosine (i.v. infusion, 140 mg·kg^{-1} min^{-1}; Sanofi-Aventis, Frankfurt am Main, Germany) and the measurements of the transit time were repeated as described above. The CFR was calculated from the ratio between the baseline and hyperaemic values.

FFR was calculated at the same time as the CFR. Measurements of FFR and CFR were performed during normal sinus

rhythm before and 15 min after 6 h of pacing. Baseline values were comparable to previous reports obtained in pigs (sham: FFR 0.97 ± 0.03), in which it was shown that CFR values (sham: 1.3 ± 0.17) are often lower than 2 and show a larger variability compared with humans (Fearon *et al.*, 2003; Kern *et al.*, 2006). There were no differences at baseline for mean FFR (D 0.92; RAP 0.93; RAP/D 0.97; RAP/A 0.87) and CFR in the groups (mean CFR: dronedarone 1.24; RAP 1.49; RAP/D 1.35; RAP/A 1.25). For comparison of FFR and CFR changes throughout the study, relative changes were calculated in comparison to baseline for each group, as in an earlier publication (Goette *et al.*, 2009).

Western immunoblotting

Samples of left ventricular tissue were frozen in liquid nitrogen and stored at –80°C. Sample preparation was performed as described by Goette *et al.*, (2009). Protein samples of 20 µg each were separated by SDS-PAGE and transferred to polyvinylidene fluoride membranes. The membranes were incubated with primary antibody against PKC-α (1:1000; Santa Cruz Biotechnology, Santa Cruz, CA, USA), phospho-PKC-α (1:1000; Cell Signaling, Danvers, MA, USA), the NADPH oxidase subunits, NOX-1 (1:500, Santa Cruz), NOX-4 (1:500, Santa Cruz), NOX-2 (1:500, BD Transduction Laboratories, San Jose, CA, USA), phospho-IκB (1:500, Cell Signaling), GAPDH (1:2000, Millipore, Temecula, CA, USA), followed by incubation with an appropriate horseradish peroxidase-conjugated secondary antibody and detection using enhanced chemiluminescence (Pierce, Rockford, IL, USA). The protein expression was quantified using AlphaEaseFC software (AlphaImager System, Alpha Innotech, San Leandro, CA, USA).

Determination of tissue concentrations of F_2-isoprostanes

Frozen left ventricular samples were homogenized by Ultra Turrax and Dounce homogenizers to yield 10% homogenates in buffer (180 mM KCl, 10 mM EDTA, 0.1 M butyl hydroxytoluene, pH 7.4). To hydrolyse esterified F_2-isoprostanes, the heart homogenates (100 µL) were treated with 4 M KOH at 40°C for 30 min and neutralized by the addition of 4 M HCl (pH adjusted to 2.0 with 0.1 M HCl). The internal standard was 9α,11 α-PGF_2 α-d_4 (1 ng; Cayman Chem. Co., Ann Arbor, MI, USA). The samples were centrifuged at 5000× *g* for 15 min, and the supernatant was applied to a C18 cartridge. Solid-phase extraction and derivatization steps were performed as previously described (Wiswedel *et al.*, 2004). F_2-isoprostanes were separated and measured by gas chromatography negative-ion chemical ionization mass spectrometry assay (DSQ/Trace GC Ultra, Thermo Fischer Scientific, Dreieich, Germany) with ammonia as reagent gas using selected ion monitoring of the carboxylate anion [M-181] at *m/z* 569 and *m/z* 573 for F2-isoprostanes and the deuterated internal standard. All analyses were performed in triplicate for each tissue sample. The protein content was determined using the method of Bradford (Bradford, 1976).

PCR and expression analysis of oxidative stress/ischaemia-related genes

Total RNA was extracted from the left ventricular samples by performing a modified phenol extraction using the Trizol reagent (Invitrogen, Karlsruhe, Germany). The prepared RNA was further purified using the Norgen's RNA Clean-Up and Concentration Micro Kit, Canada. Concentration of the purified RNA preparations was measured using the NanoDrop ND-1000 spectrophotometer (Thermo Fisher Scientific Inc, Dreieich, Germany). RNA purity was determined by calculating the 260/280 nm and 260/230 nm ratios. The RNA quality was assessed using the lab-on-chip capillary electrophoresis technology (Bioanalyzer 2100, Agilent Technologies, Santa Clara, CA, USA). Only RNA samples with an RNA Integrity Number higher than 7 were used for further analyses.

To identify global changes in gene expression, transcriptome analyses were performed. Target RNA labelling and hybridization was accomplished according to the manufacturer's protocol (GeneChip® 3′ IVT Express Kit user manual, Affymetrix, Inc., Santa Clara, CA, USA) using 200 ng of total RNA per sample. The chips were washed and stained with a GeneChip Fluidics Station 450 (Affymetrix, Inc.) using the standard fluidics protocol. Chips were then scanned with an Affymetrix GeneChip Scanner 3000 (Affymetrix, Inc.). Microarray data analysis was done using the Rosetta Resolver® system for gene expression data analysis (Rosetta Biosoftware, Seattle, WA, USA) by processing the Affymetrix CEL files using the Affymetrix Rosetta intensity data summarization. The pathway and functional analysis of the differentially expressed genes was carried out using the commercial system biology oriented package Ingenuity Pathways Analysis and using the annotation details provided by Christopher K. Tuggle (Couture *et al.*, 2009).

Quantitative PCR was performed as described recently (Goette *et al.*, 2009) using the CFX960 (Bio-Rad, Munich, Germany) and the specific primers given in (Table 1). Quantities of GAPDH mRNA were used to normalize cDNA contents. Values are given in arbitrary units.

HL1 cell in vitro *experiments*

The murine cardiomyocyte cell line HL1 (kindly provided by Dr. William Claycomb, Louisiana State University Health Science Center, New Orleans, LA) was used for *in vitro* experiments. Cells were passaged and cultured in Claycomb-Medium (Sigma-Aldrich, Taufkirchen, Germany) as described (Claycomb *et al.*, 1998).

HL1 cells were subjected to continuous oxidative stress by adding glucose oxidase (GOD) and glucose to the culture medium. Briefly, cells were seeded into 96-well plates at a density of 4×10^4 cells per well in 200 µL of medium. After 24 h, medium was replaced by fresh medium, supplemented with 5.5 mM glucose and different concentrations of GOD (from *Aspergillus niger*, Sigma-Aldrich). 2′,7′-Dichlorodihydrofluorescein diacetate (24 µM; Sigma-Aldrich) was added to the culture medium, and fluorescence intensity was read at 488 nm excitation wavelength and 520 nm emission wavelength after 2 h to quantify reactive oxygen species (ROS) production.

To determine the effects of amiodarone or dronedarone on oxidative stress-dependent PKCα-activation, HL1 cells were seeded into 6-well plates at a density of 1×10^6 per well in 3 mL medium. After 24 h, medium was replaced by fresh one containing 5 mU·mL^{-1} GOD and 5.5 mM glucose without dronedarone or amiodarone, respectively. After additional 24 h of culture, protein lysates for immunoblot analy-

Table 1
Primers used for quantitative RT-PCR

Gene	Primer sequence	Product size (bp)
CCL2	US: 5′-CTG CTC ACT GCA GCC ACC TTC	398
	DS: 5′-GGC ATC ATG TTT CGT ATC	
DNAJB9	US: 5′-CAG GAT GGT TCC AGT AGA C	235
	DS: 5′-GTC CTG AAC AGT CAG TGT ATG	
HIF-1α	US: 5′- GAG AAG TCT AGA GAT GCA GC	255
	DS: 5′- CAC CAT CAT CTG TGA GTA CC	
PRKAG2	US: 5′-CTC TTC GAT GCT GTA CAC TC	377
	DS: 5′-GTC ACC GTG ATG TCT AGG TTG	
Prx1	US: 5′-CTC CGT GGA TGA GAC TCT GAG	261
	DS: 5′-GTC CCA CAC ATC TGA GCT G	
Prx3	US: 5′-CTT GAC AAG TGT GCT GTG GTC	416
	DS: 5′-CTA ACA GCA CAC CGT AGT CTC	
PPARGC1	US: 5′-GAT GCA CTG ACA GAT GGA GAT G	388
	DS: 5′-GTG CAC TTG TCT CTG CTA CTG	
PRKCα	US: 5′-GTG ACA CCT GTG ACA TGA AC	365
	DS: 5′-GTT CCT TGT TGT TCG GTC	
VEGF-A	US: 5′-CTC CAC CAT GCC AAG TGG TC	289
	DS: 5′-CTC ATC TCT CCT ATG TGC TG	
β-actin	US: AAG ATG ACC CAG ATC ATG TTT GAG	648
	DS: AGG AGG AGC AAT GAT CTT GAT CTT	

US, upstream primer; DS, downstream primer.

ses were prepared using TriFast (Peqlab, Erlangen, Germany) following the protocol recommended by the supplier.

Rapid pacing *in vitro* of HL-1 cells (6-well plates, 1×10^6 cells per well in 4 mL) was performed with carbon electrodes using the culture cell pacer system C-Pace EP (IonOptix, Milton, MA, USA). Cells were paced at 20 Hz for 7 or 24 h (5 $V \cdot cm^{-1}$, 4 msec bipolar pulse).

Data analysis

The values summarized in Tables 2 and 3 are given as median with first and third quartile. Haemodynamic parameters represent averaged values from repetitive measurements within each animal throughout the study period. Kruskal–Wallis test was performed to determine any differences between the groups (sham; RAP; RAP/D; RAP/A; D) at baseline and after 6 h pacing as well as the time-dependent changes within these groups (Tables 2 and 3). Time-dependent changes were calculated as (6 h value-baseline value)/baseline value. When there was a significant Kruskal–Wallis test, the Mann–Whitney test was used for pairwise group comparison. Measurements of FFR and CFR were performed during normal sinus rhythm before and 15 min after 6 h pacing (end of experiment). Protein, mRNA expression and F_2-isoprostane data were also analysed using Kruskal–Wallis test and Mann–Whitney test. The values are shown as medians with box (1st and 3rd quartile) and whisker (range) plots. Data from transcriptome analyses were analysed using one-way ANOVA as the established standard procedure for this type of analysis; values are expressed as mean ± SD. All statistical decisions were made two-tailed with a critical probability of $\alpha = 5\%$ without α-adjustment. Statistical analyses were performed using IBM® SPSS® Statistics 18 (IBM Corporation, Somer, NY, USA).

Results

Haemodynamic parameters, FFR and CFR

There were no statistically significant differences in haemodynamic parameters (Table 2) as well as FFR/CFR and electrophysiological parameters (Table 3) between the four groups at baseline. FFR was comparable between groups at baseline (Table 3) but was different after 6 h of pacing. There were no changes in the FFR in the sham, RAP and RAP/D and dronedarone groups (Figure 1, upper panel). In comparison to these groups, RAP/A showed reduced FFR values after 6 h. However, FFR remained above 0.8 and, therefore, significant obstruction of blood flow was not present. CFR, which is a combined measure of flow reserve in the epicardial arteries and the microcirculation, was similarly comparable across the groups at baseline (Table 3). CFR was decreased in the RAP and RAP/A group, but was higher in RAP/D- and dronedarone-treated animals (Figure 1, lower panel). The results suggest that there is microcirculatory disturbance during pacing

Table 2

Haemodynamic parameters at baseline and after 6h and time-dependent effect

Parameter	Time	Sham ($n = 6$) Median (Q_1; Q_3)	RAP ($n = 6$) Median (Q_1; Q_3)	RAP/D ($n = 6$) Median (Q_1; Q_3)	D ($n = 7$) Median (Q_1; Q_3)	*P*-value (Kruskal–Wallis)
Hemodynamic parameters						
RA systolic pressure (mmHg)	Baseline	6.50 (3.00; 10.00)	6.50 (6.00; 8.00)	7.00 (4.00; 9.00)	7.00 (5.50; 7.00)	0.955
	At 6 h	8.00 (5.00; 12.00)	8.00 (7.00; 10.00)	10.00 (7.00; 11.00)	10.00 (8.50; 10.50)	0.715
RA systolic pressure effect [(6 h-baseline)/baseline)]	n.a.	–0.08 (–0.43; 0.33)	0.14 (–0.13; 0.67)	0.49 (0.43; 0.75)	0.57 (0.50; 0.63)	0.356
RV systolic pressure (mmHg)	Baseline	25.00 (23.00; 28.00)	24.00 (23.00; 26.00)	25.00 (24.00; 26.00)	24.00 (22.00; 26.50)	0.868
	At 6 h	27.00 (27.00; 27.00)	26.50 (24.00; 32.00)	28.50 (25.00; 35.00)	24.00 (22.50; 27.50)	0.391
RV systolic pressure effect [(6 h-baseline)/baseline)]	n.a.	0.13 (0.08; 0.17)	0.06 (0.00; 0.13)	0.07 (0.04; 0.46)	0.00 (–0.02; 0.06)	0.569
Aortic systolic pressure (mmHg)	Baseline	75.00 (71.00; 81.00)	80.00 (79.00; 87.00)	72.00 (67.00; 88.00)	75.00 (72.00; 79.00)	0.359
	At 6 h	75.00 (66.00; 82.00)	78.50 (62.00; 81.00)	76.00 (72.00; 80.00)	63.00 (62.50; 69.00)	0.247
Aortic systolic pressure effect [(6 h-baseline)/baseline)]	n.a.	–0.04 (–0.16; 0.01)	0.01 (–0.22; 0.03)	0.02 (–0.06; 0.14)	–0.13 (–0.17; –0.06)	0.296
Aortic diastolic pressure (mmHg)	Baseline	45.00 (35.00; 50.00)	47.00 (44.00; 60.00)	40.00 (39.00; 48.00)	50.00 (45.00; 51.50)	0.182
	At 6 h	43.00 (33.00; 53.00)	42.00 (41.00; 61.00)	44.00 (40.00; 51.00)	42.00 (40.50; 44.50)	0.962
Aortic diastolic pressure effect [(6 h-baseline)/baseline)]	n.a.	–0.07 (–0.17; 0.06)	0.03 (–0.30; 0.38)	0.06 (–0.05; 0.31)	–0.17 (–0.20; –0.02)	0.411
BP systolic (mmHg)	Baseline	78.00 (71.00; 83.00)	84.00 (81.00; 92.00)	75.00 (72.00; 83.00)	81.00 (74.50; 84.00)	0.343
	At 6 h	77.00 (70.00; 94.00)	82.00 (81.00; 91.00)	82.00 (68.00; 87.00)	70.00 (67.50; 74.50)	0.163
BP systolic effect [(6 h-baseline)/baseline)]	n.a.	–0.07 (–0.15; 0.18)	0.01 (–0.11; 0.12)	0.01 (–0.10; 0.20)	–0.11 (–0.15; –0.06)	0.484
BP diastolic baseline (mmHg)	Baseline	46.50 (43.00; 53.00)	55.00 (46.00; 61.00)	47.50 (44.00; 51.00)	52.00 (48.50; 52.50)	0.393
	At 6 h	49.00 (47.00; 65.00)	58.00 (41.00; 73.00)	56.50 (42.00; 57.00)	43.00 (40.50; 47.50)	0.207
BP diastolic baseline effect [(6 h-baseline)/baseline)]	n.a.	0.08 (–0.10; 0.11)	–0.04 (–0.24; 0.59)	0.14 (0.02; 0.19)	–0.13 (–0.17; –0.09)	0.072
LV end-diastolic pressure (mmHg)	Baseline	3.50 (2.00; 7.00)	4.00 (2.00; 4.00)	4.00 (2.00; 8.00)	4.00 (2.00; 7.50)	0.892
	At 6 h	5.00 (5.00; 5.00)	0.00 (0.00; 4.00)	3.50 (2.00; 5.00)	2.00 (2.00; 6.00)	0.097
LV end-diastolic pressure effect [(6 h-baseline)/baseline)]	n.a.	0.00 (–0.21; 1.50)	–0.50 (–1.00; 0.00)	–0.13 (–0.38; 0.00)	–0.21 (–0.50; 0.00)	0.582
Mean heart rate (b.p.m.)	Baseline	94.50 (91.00; 98.00)	96.00 (94.00; 102.00)	91.00 (86.00; 116.00)	88.00 (85.00; 99.50)	0.598
	At 6 h	90.00 (80.00; 113.00)	127.50 (115.00; 156.00)	113.50 (101.00; 142.00)	96.00 (88.00; 113.50)	0.106
Mean heart rate effect [(6 h-baseline)/baseline)]	n.a.	–0.06 (–0.12; 0.15)	0.25 (0.17; 0.64)	0.27 (0.11; 0.35)	0.08 (–0.14; 0.22)	0.290

Q_1, 1st quartile; Q_3, 3rd quartile; RA, right atrium; RV, right ventricle; BP, blood pressure; LV, left ventricular; n.a., not applicable.

Table 3

Flow markers and electrophysiological parameters at baseline and at 15 min after 6h RAP and time-dependent effect

Parameter	Time	Sham ($n = 6$) Median (Q_1; Q_3)	RAP ($n = 6$) Median (Q_1; Q_3)	RAP/D ($n = 6$) Median (Q_1; Q_3)	D ($n = 7$) Median (Q_1; Q_3)	*P*-value (Kruskal–Wallis)
Flow markers						
FFR	Baseline	0.96 (0.94; 1.00)	0.913 (0.90; 0.94)	0.96 (0.94; 1.00)	0.93 (0.87; 0.97)	0.091
	At 6 h	0.93 (0.89; 0.98)	0.86 (0.83; 0.90)	0.93 (0.90; 0.96)	0.97 (0.97; 1.00)	0.043
FFR time-dependent effect [(6 h-baseline)/baseline]	n.a.	0.01 (–0.11; 0.04)	–0.07 (–0.11; 0.01)	–0.02 (–0.07; 0.01)	0.08 (–0.01; 0.12)	0.088
CFR	Baseline	1.25 (1.20; 1.30)	1.40 (1.40; 1.50)	1.30 (1.20; 1.60)	1.20 (1.15; 1.35)	0.135
	At 6 h	1.30 (1.30; 1.30)	0.80 (0.70; 1.00)	1.35 (1.20; 1.40)	1.30 (1.25; 1.50)	0.007
CFR time-dependent effect [(6 h-baseline)/baseline]	n.a.	0.08 (0.00; 0.08)	–0.43 (–0.50; –0.39)	–0.07 (–0.09; 0.00)	0.08 (–0.03; 0.22)	0.002
Electrophysiological parameters						
ERP (ms)	Baseline	220 (180; 240)	220 (200; 220)	245 (200; 250)	220 (210; 235)	0.750
	At 6 h	225 (200; 250)	170 (150; 185)	225 (220; 240)	235 (210; 250)	0.034
ERP time-dependent effect [(6 h-baseline)/baseline]	n.a.	0.08 (0.04; 0.11)	–0.19 (–0.20; –0.18)	0.03 (–0.04; 0.35)	0.00 (–0.04; 0.04)	0.027
QTc (ms)	Baseline	386 (374; 403)	357 (347; 379)	389 (351; 407)	371 (363; 381)	0.182
	At 6 h	416 (408; 476)	354 (331; 360)	384 (336; 392)	410 (378; 442)	0.011
QTc time dependent effect [(6 h-baseline)/baseline]	n.a.	0.09 (0.07; 0.29)	–0.00 (–0.04; 0.00)	–0.04 (–0.04; –0.02)	0.13 (0.03; 0.15)	0.043

Q_1, 1st quartile; Q_3, 3rd quartile; LV, left ventricular; FFR, fractional flow reserve; CFR, coronary flow reserve; ERP, effective refractory period; n.a., not applicable.

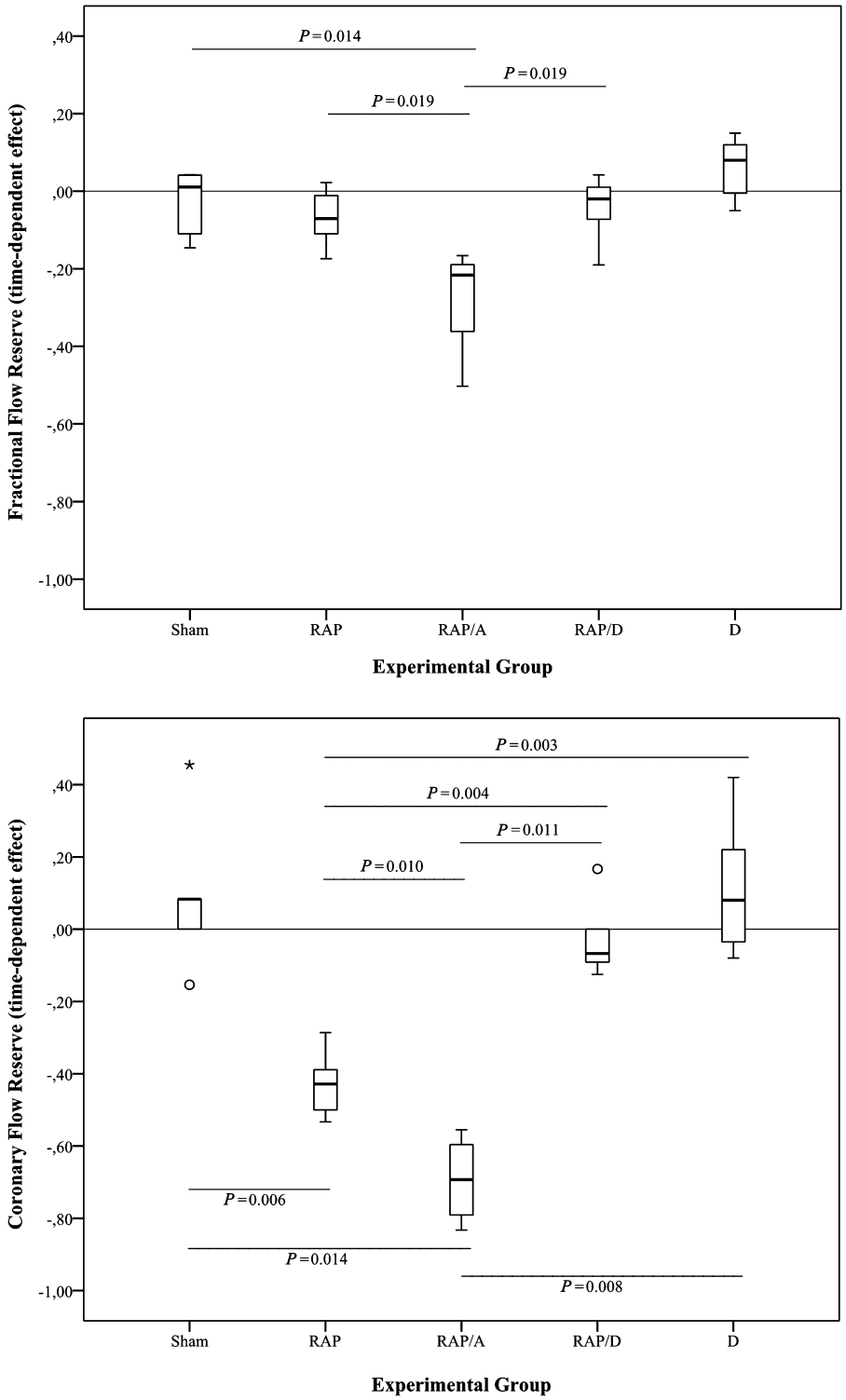

Figure 1

The upper panel shows the effects of dronedarone (D) or amiodarone (A) on epicardial coronary artery flow (FFR) after RAP and the lower panel, the effects of dronedarone or amiodarone on CFR after RAP. Results are expressed as the ratio between values obtained after RAP for 6h and those obtained before the RAP procedure. In this Figure and in other similar Figures, data are shown as medians with box (1st and 3rd quartiles) and whisker (range) plots. Differences between data sets, with P values, are indicated; Kruksal-Wallis followed by Mann Whitney post test. ●, outlier; *, extreme value.

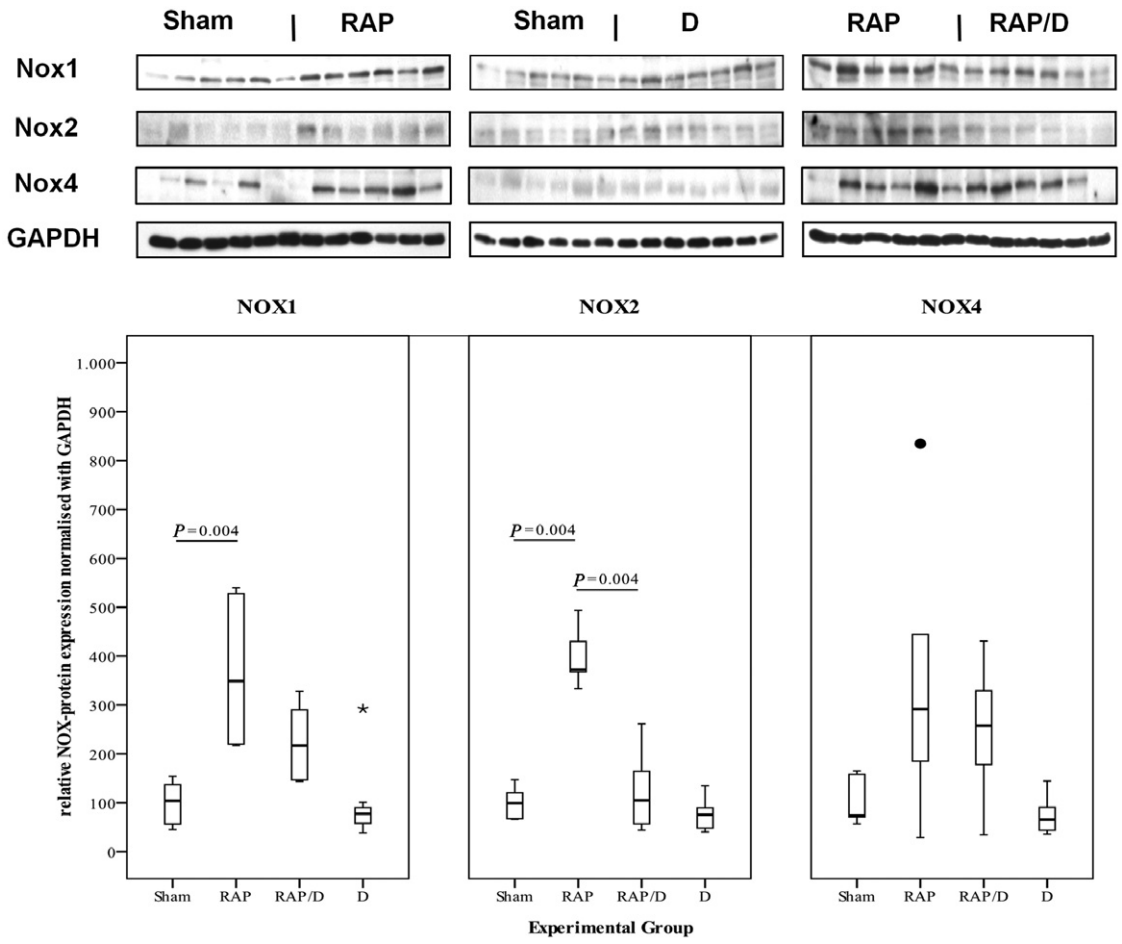

Figure 2

Effect of dronedarone (D) on NADPH oxidase subunit (NOX) isoforms 1, 2 and 4 protein, assessed by Western blots, in the left ventricle after RAP. Results shown are the changes, induced by treatments, in the NOX : GAPDH ratio; sham ratios were set to 100. Data are shown and analysed as described in Figure 1. ●, outlier; *, extreme value.

which was reversed by dronedarone. Figure 1 (lower panel) also illustrates that amiodarone did not affect the reduction of CFR induced by RAP.

NADPH oxidase subunit (NOX) isoforms 1, 2, 4

NADPH oxidase is a major source of ROS in cardiac tissue and this enzyme generates constitutively low levels of intracellular ROS, which can be up-regulated in pathological settings. NOX is the key catalytic subunit of NADPH oxidase, and the expression of NOX family members was analysed under study conditions. Figure 2 illustrates the up-regulation of NOX 1 and NOX 2, compared with sham levels, after 6 h RAP. Dronedarone clearly reduced this RAP-induced up-regulation of NOX 2 and there was a similar but not significant ($P = 0.15$) effect on NOX 1.

Left ventricular F_2-isoprostane concentrations

To evaluate if the observed RAP-dependent increase of NADPH oxidase was associated with increased amounts of oxidative stress markers, left ventricular concentrations of F_2-isoprostanes were determined. The level of F_2-isoprostanes was elevated by 76% after RAP compared with sham, and was significantly reduced in the RAP/D group (Figure 3). This indicates that dronedarone reduced oxidative stress.

Phosphorylation of PKC

PKC has been shown to contribute to the phosphorylation and, thus, activity of NOX subunits. The isoform PKCα is itself activated by phosphorylation. Figure 4 illustrates that phosphorylation of PKCα was increased during RAP, compared with sham. There was a very marked trend towards inhibition by dronedarone of this RAP-induced effect, which almost reached significance ($P = 0.055$).

Redox-sensitive transcription factor

In response to oxidative stress, there is a rapid activation of redox-sensitive signalling molecules such as the transcriptional factor NF-κB. The first step in the activation of NF-κB is the phosphorylation of its endogenous inhibitor, inhibitor of nuclear factor of kappa light chain gene enhancer in B-cells alpha (IκBα), on serine residues in its N-terminal regulatory

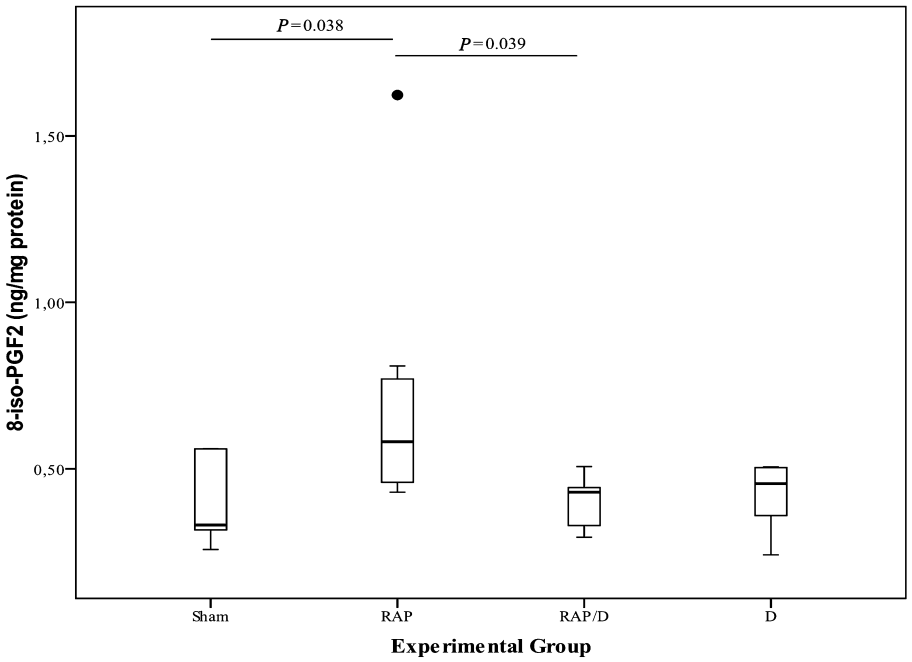

Figure 3

Effect of RAP and dronedarone (D) on F_2-isoprostane levels in left ventricular tissue. Samples were taken 15min after the end of RAP for 6h and F_2-isoprostanes measured by GC-MS. Data are shown and analysed as described in Figure 1. ●, outlier.

Table 4

Change of gene expression level (microarray data) in left ventricular tissue, taken from sham, RAP and RAP/D groups

Glycogen metabolism/ stress related	Sham vs. RAP (n = 4)		RAP vs. RAP/D (n = 6)	
	Fold change	P-value (ANOVA)	Fold change	P-value (ANOVA)
HK2	7.8	0.001	–1.7	N.S.
GSK3B	1.6	0.25	1.2	N.S.
PYGM	–1.4	0.08	1.1	N.S.
VEGF-A	1.6	0.03	–1.3	N.S.
CCL2	2.2	0.005	–1.9	N.S.
PRKAG2	3.5	<0.001	–1.3	N.S.
PPARGC1A	3.4	<0.001	–1.4	N.S.
ACADL	–1.3	0.12	1.1	N.S.
HIF1A	–1.2	N.S.	–1.2	N.S.

HK2, hexokinase 2; GSK3B, glycogen synthase kinase 3β; PYGM, muscle isoform of glycogen phosphorylase; AGL, anti-glycogen debranching enzyme; PRKAG2, PKA subunit γ-2; PPARGC1A, PPARγ coactivator 1-α; ACADL, acyl-coenzyme A dehydrogenase locus; HIF1A, hypoxia-induced factor-1α.

domain. As shown in Figure 5, there was increased phosphorylation of IκBα in the RAP group, compared with the sham group, which was prevented by dronedarone.

Alterations of ischaemia-related genes and glycogen metabolism

A comprehensive assessment of the expression of genes related to ischaemia and glycogen metabolism, by whole genome transcriptome analysis is shown in Table 4. It illustrates that in response to 6 h of RAP, there were significant changes in gene expression, indicating oxidative stress/ischaemia. The functional categories of the genes included glycogen metabolism (hexokinase 2, glycogen synthase kinase (GSK) 3β, the muscle isoform of glycogen phosphorylase), hypoxia/ischaemia [hypoxia-inducible factor-1α (HIF-1α), VEGF-A, PPARγ coactivator 1-α (PPARGC1)] and oxidative stress [DnaJ homolog family members, peroxire-

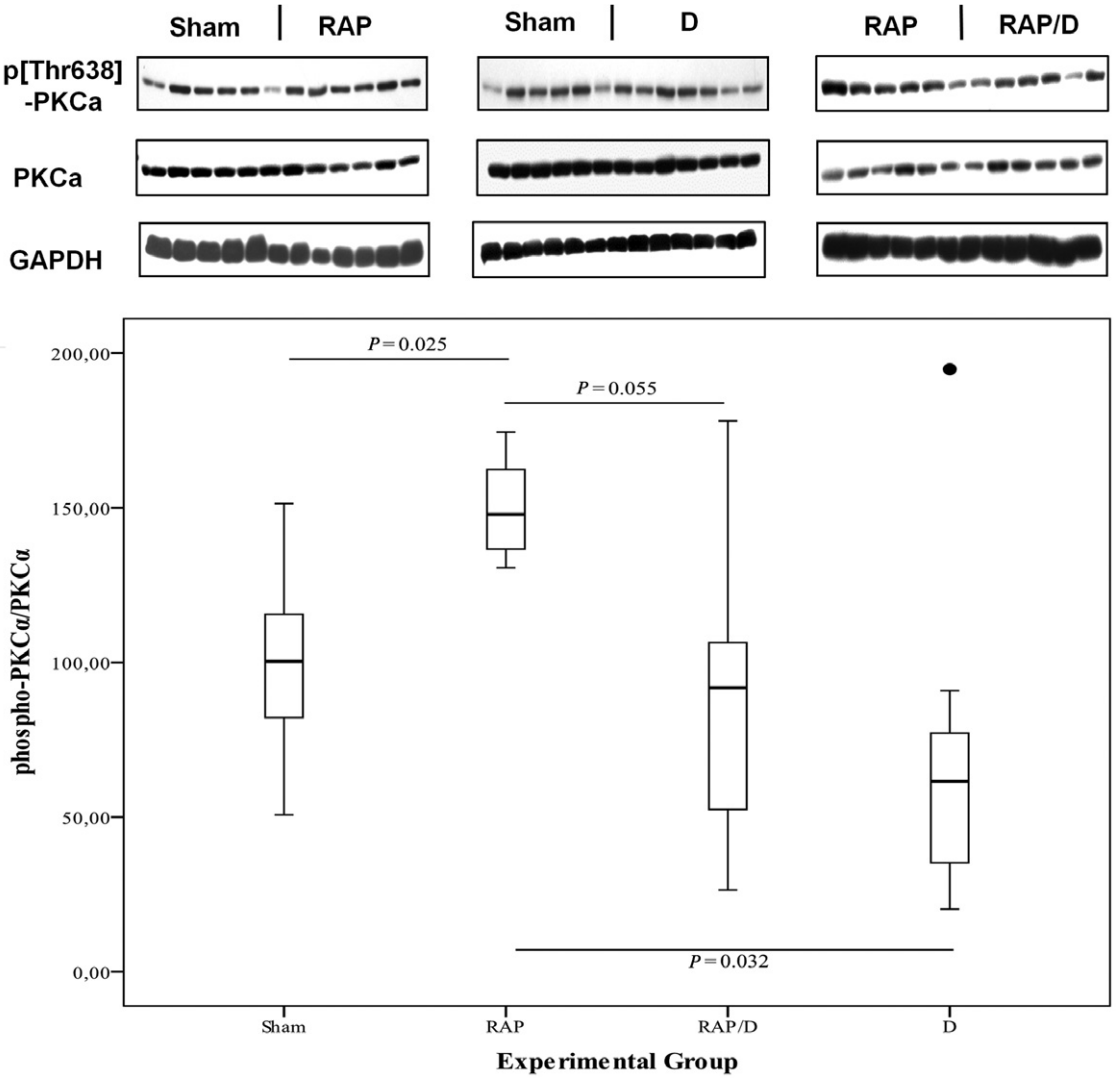

Figure 4

Effect of dronedarone (D) on phosphorylation of Thr^{638} in PKCα in left ventricular tissue after RAP. Data are shown and analysed as described in Figure 1. ●, outlier.

doxins (Prxs), the chemokine CCL-2]. Dronedarone treatment did not significantly attenuate these RAP-induced changes.

Oxidative stress/ischaemia-related genes

Following the results from the microarray analyses, the expression mRNA from oxidative stress/ischaemia-related genes was analysed in left venrtricular samples by quantitative real time-PCR (RT-PCR) (Table 5). RAP significantly increased mRNA from VEGF-A, PKA subunit γ-2 (PRKAG2), DnaJ homologue subfamily B member 9 and Prx3 and showed a trend towards increasing that from PPARGC1, compared with levels in samples from the sham group. Treatment with dronedarone significantly reduced this RAP-dependent increase of mRNA from VEGF-A, PRKAG2, PPARGC1 and the gene encoding the chemokine CCL2. In contrast to dronedarone, amiodarone was not able to prevent the RAP-dependent increase in CCL2, but led to a further increase and amiodarone was also less effective in attenuating the RAP-dependent induction of mRNA from PPARGC1 (Table 5).

HL1 in vitro *experiments*

To confirm the effects of direct oxidative stress or RAP on the activation of PKCα and its sensitivity to amiodarone or dronedarone *in vitro*, the murine cardiomyocyte cell line HL1 was used. Exposure of HL1 cells to a combination of glucose oxidase (GOD) with its substrate, glucose, dose-dependently increased production of H_2O_2, providing a model of oxidative stress (Figure 6A). Using an intermediate concentration of GOD (5 mU·mL^{-1}), we showed that in response to direct oxidative stress, there was a ROS-dependent, 1.6-fold increase in PKCα activation which was prevented by dronedarone (Figure 6B). Amiodarone did not have a similar effect.

In response to 7 h of rapid pacing in vitro, there was also a significant increase in the extent of phosphorylation of PKCα observed. This RAP-dependent increase in pPKCα was

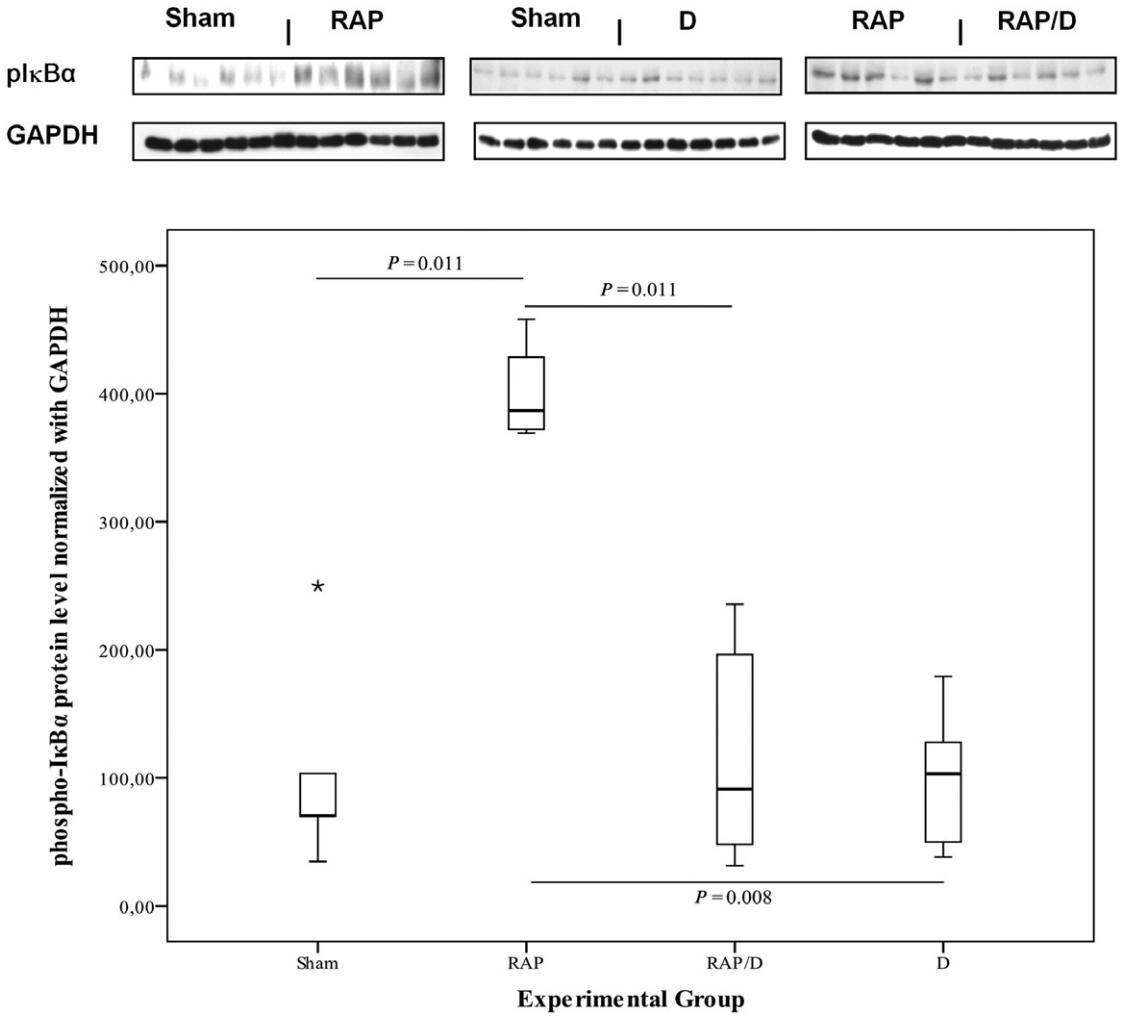

Figure 5

Effect of dronedarone (D) on phosphorylation of IκBα in left ventricular tissue after RAP. Results shown are the changes, induced by treatments, in the pIκBα : GAPDH ratio; sham ratios were set to 100. Data are shown and analysed as described in Figure 1. * extreme value.

hardly affected by amiodarone, whereas dronedarone exhibited a strong tendency to decrease amounts of pPKCα (P = 0.059) (Figure 6C). The direct comparison of the efficacy of dronedarone and amiodarone to attenuate RAP-dependent phosphorylation of PKCα revealed a significantly higher potency of dronedarone (P = 0.021).

Over a range of concentrations, neither dronedarone nor amiodarone showed a clear effect on PKCα phosphorylation in HL1 cells, under basal conditions. There appeared to be a tendency of dronedarone at higher concentrations to decrease the amounts of phospho-PKCα, but this was not consistently observed (Figure 6D).

Discussion

Our results show that dronedarone reduced microvascular abnormalities and oxidative stress induced by RAP. Dronedarone also significantly reduced expression of genes for ROS-generating enzymes (NAPDH oxidase) and oxidative stress response proteins (PKC, NF-κB). Our findings provide a possible explanation of the reduction in the incidence of acute coronary events in patients with AF, treated with dronedarone (Connolly *et al.*, 2011).

Microcirculatory flow abnormalities in AF

Recent studies have shown that patients with AF show ventricular flow abnormalities and a high incidence of cardiac events (Abidov *et al.*, 2004; Range *et al.*, 2007). Consistent with these, myocardial blood flow is substantially reduced in AF while coronary artery resistance is elevated (Range *et al.*, 2007). These findings are supported by an increase in the Doppler-derived coronary vascular resistance index, observed in experimental models of AF (Kochiadakis *et al.*, 2002). The present experiments showed that RAP reduced CFR but not FFR, an effect abolished by dronedarone but not amiodarone indicating the prevention of RAP-induced ventricular microcirculatory flow disturbances. This has not been previously

Table 5
mRNA expression levels of oxidative stress related genes (determined by quantitative RT-PCR)

	Sham (n = 5) Median (Q1; Q3)	RAP (n = 6) Median (Q1; Q3)	RAP/D (n = 6) Median (Q1; Q3)	D (n = 7) Median (Q1; Q3)	RAP/A (n = 4) Median (Q1; Q3)	P-value (Kruskal–Wallis)	P-value (Sham vs. RAP)	P-value (RAP vs. RAP/D)	P-value (RAP vs. RAP/A)	P-value (RAP/D vs. RAP/A)	P-value (Sham vs. D)	P-value (RAP vs. D)
HIF-1α	106.87 (63.66; 124.55)	204.90 (153.58; 436.57)	121.39 (105.26; 129.69)	71.65 (28.51; 104.72)	91.80 (61.20; 123.00)	0.017	0.016	0.037	0.033	0.522	0.253	0.004
VEGF-A	70.50 (47.50; 93.50)	240.00 (175.00; 262.50)	53.00 (33.00; 56.00)	66.00 (59.00; 70.00)	49.94 (32.44; 63.74)	0.008	0.037	0.010	0.038	0.571	0.391	0.038
CCL2	113.50 (82.50; 130.50)	296.00 (202.00; 303.50)	74.60 (70.00; 93.00)	86.00 (59.00; 106.00)	479.33 (366.88; 647.44)	0.005	0.200	0.025	0.055	0.011	0.143	0.025
PRKAG2	87.95 (67.60; 195.20)	374.30 (311.30; 772.75)	120.20 (99.80; 158.70)	133.60 (107.00; 137.90)	157.93 (143.35; 178.32)	0.010	0.047	0.004	0.014	0.131	0.116	0.009
PRKCα	97.90 (93.40; 106.40)	236.60 (215.75; 280.50)	152.20 (107.80; 221.50)	122.30 (120.70; 122.50)	81.90 (69.57; 97.26)	0.011	0.086	0.273	0.027	0.033	0.011	0.361
DNAJB9	92.50 (78.00; 116.00)	211.00 (177.00; 317.00)	114.00 (101.00; 143.00)	77.00 (73.00; 102.00)	113.81 (97.49; 120.13)	0.004	0.008	0.055	0.011	0.394	0.423	0.004
Prx3	96.85 (81.35; 109.40)	171.10 (150.85; 221.80)	92.80 (87.50; 153.80)	90.10 (74.80; 94.10)	145.86 (144.28; 148.39)	0.01	0.037	0.116	0.394	0.257	0.046	0.007
PPARGC1	84.85 (61.20; 96.75)	267.60 (226.10; 373.90)	66.20 (48.40; 89.20)	70.80 (61.80; 85.10)	136.94 (123.72; 142.28)	0.01	0.076	0.018	0.142	0.033	0.201	0.028

HIF-1α, hypoxia-induced factor 1 α; PRKAG2, PKA subunit γ-2; PRKCα, PKC α; DNAJB9, DnaJ homolog subfamily B member 9; Prx3, peroxiredoxin 3; PPARGC1, PPARγ coactivator 1-α; Q1, 1st quartile; Q3, 3rd quartile.

reported, but the ATHENA trial suggested a beneficial role of dronedarone by reducing acute coronary events in patients with AF and concomitant CAD (Crijns *et al.*, 2009). In addition, there are direct cardioprotective effects of dronedarone, as a recent study using a pig model of ischaemia/reperfusion demonstrated a reduction of infarct size that was independent of the actual subendocardial blood flow (Skyschally and Heusch, 2011).

Mechanistic insights into the actions of dronedarone

Oxidative stress is associated with microvascular flow abnormalities and occurs immediately after new-onset AF. It may be induced by altering cellular ionic homeostasis (tachycardia-induced intracellular calcium and sodium overload). As a consequence, PKC is phosphorylated, catalytic subunits of NOX are up-regulated and ROS increased. ROS induce redox-sensitive protein kinases which in turn activate NF-κB (Schreck *et al.*, 1992; Flohe *et al.*, 1997; Lee *et al.*, 1999; Bowie and O'Neill, 2000; Rahman, 2003). NF-κB appears to be a key mediator of ROS-induced inflammatory effects, leading to increased expression of adhesion molecules and inflammatory gene products in vascular cells (Alexander, 1995; Berliner *et al.*, 1995). Among the subcellular targets of NF-κB is HIF-1α, which is activated by ROS via a functional NF-κB site (Bonello *et al.*, 2007). HIF-1 α in turn activates expression of VEGF (Forsythe *et al.*, 1996). Further genes activated by NF-κB include those for CCL2 (Lawrence *et al.*, 2006) and VEGF (Kiriakidis *et al.*, 2003) (Table 5). In our experiments, oxidative stress-related intracellular signalling and gene transcription was increased, as exemplified by increased PKC phosphorylation, NADPH isoform expression, isoprostane release, IκBα phosphorylation and induction of a panel of oxidative stress-related genes. A functional correlate is the reduction of CFR, observed *in vivo*.

Panel of oxidative stress-related genes

Oxidative stress is increased during AF and has been implicated in the pathogenesis of AF (Carnes *et al.*, 2001; Mihm *et al.*, 2001; Korantzopoulos *et al.*, 2007; Huang *et al.*, 2009). Increased expression and activity of NADPH oxidase (Kim *et al.*, 2008) contributes to ROS production during AF. Also Kim *et al.*, (2003) observed an increased mRNA expression of ROS-producing and anti-oxidative genes. To confirm the association of flow abnormalities with RAP-dependent induction of oxidative stress-related gene expression and to assess any protective effects of treatment with dronedarone, the expression of these genes was assessed in left ventricular tissue by quantitative RT-PCR. ROS are known to act as intracellular messengers leading to the activation and nuclear translocation of the redox-sensitive transcription factor NF-κB, and consequent expression of the genes VEGF-A (Kiriakidis *et al.*, 2003; Martin *et al.*, 2009), CCL2 (Lawrence *et al.*, 2006) and HIF1A (Kunsch and Medford, 1999; Bonello *et al.*, 2007), as well as those for the DnaJ family proteins.

PRKAG2 and VEGF-A are closely associated with changes in the calcium signalling and thus play a role in the production of NO in the vascular system by endothelial NO synthase (eNOS), a Ca^{2+}/calmodulin-dependent enzyme. NO reacts with ROS, especially superoxide, to produce reactive species

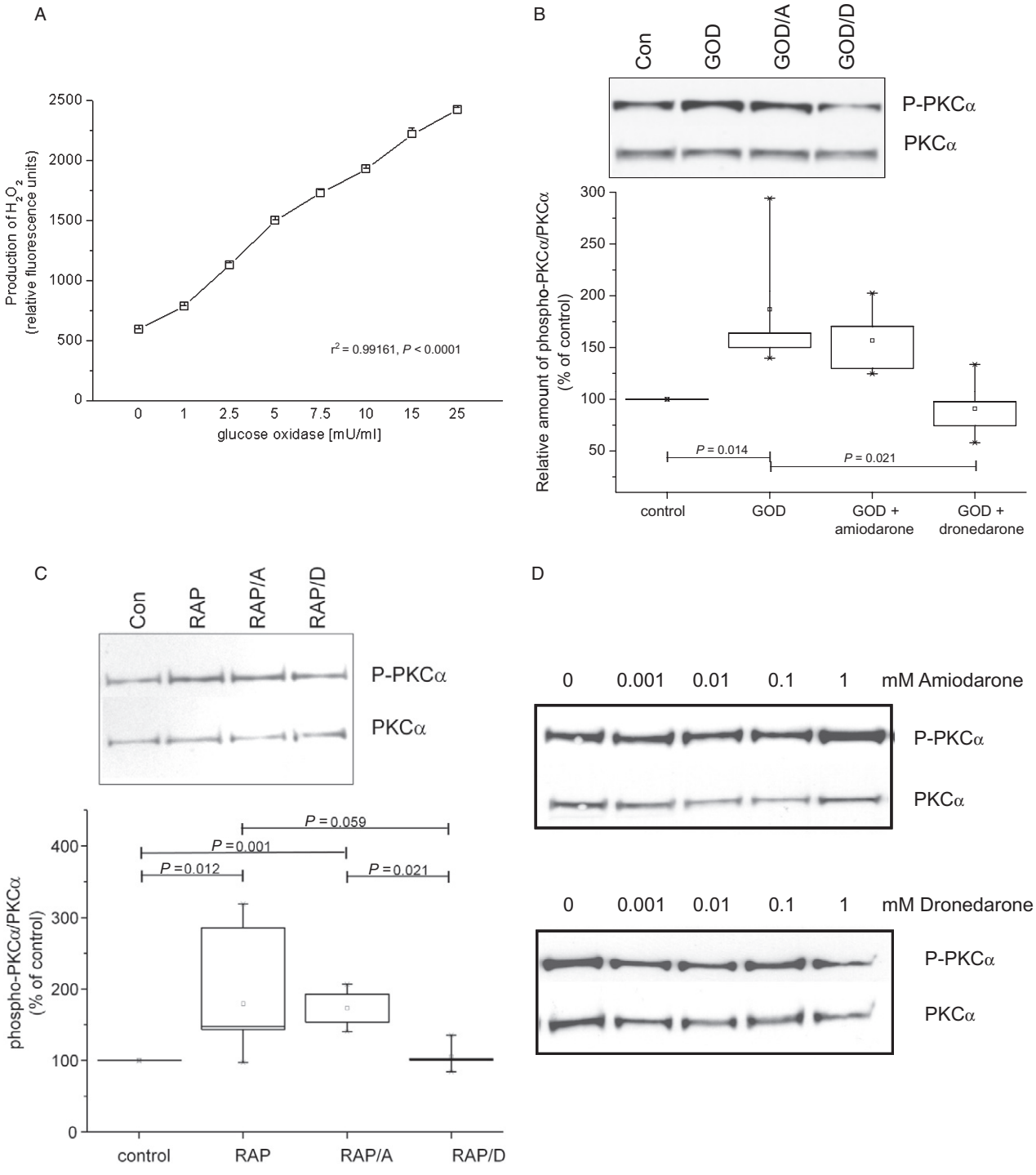

Figure 6

Dronedarone attenuates oxidative stress-induced and RAP-dependent activation of PKCα in HL1 cardiomyocytes *in vitro*. (A) Exposure of HL1 cells to glucose oxidase (GOD) and 5.5 mM glucose dose-dependently increased production of H_2O_2 ($n = 6$). (B) In HL1 cells increased oxidative stress, from GOD (5mU mL^{-1}) + glucose(5mM) led to increased phosphorylation of PKCα, which was reduced by dronedarone but not amiodarone (n = 4). Results are shown relative to control (set to 100). Data are shown and analysed as described in Figure 1. (C) Rapid pacing *in vitro* also increased the amounts of phosphoPKCα. Dronedarone showed a marked tendency ($P = 0.059$) to inhibit this increase ($n = 4$). Results are shown relative to control (set to 100). Data are shown and analysed as described in Figure 1. (D) Neither dronedarone nor amiodarone affected phosphorylation of PKCα under basal conditions.

peroxynitrite ($OONO^-$), thereby reducing NO bioavailability and elevating vascular resistance and promoting vasoconstriction (Dusting *et al.*, 1998; Dusting and Dart, 1999; Zicha *et al.*, 2001). As a result, expression of the anti-oxidant Prxs is induced (Wolf *et al.*, 2010). PPARGC1, a multifunctional coactivator involved in the regulation of cardiac mitochondrial functional capacity and cellular energy metabolism, has recently been shown to accelerate cytosolic Ca^{2+} clearance in cardiac myocytes (Chen *et al.*, 2010). NO may also act to suppress the vascular NADPH oxidase activity, which is a major source of oxidative stress (Dusting *et al.*, 2005).

Recent evidence indicates that besides HIF-1α, a key component of the eukaryotic oxygen-response system, other factors are crucially involved in the regulation of oxidative (metabolic) programs. One of these pathways involves PPARGC1 (Shoag and Arany, 2010). Expression of PPARGC1 is induced by ROS and acts protectively by increasing the expression of ROS-limiting and scavenging genes including Prx3 (Valle *et al.*, 2005; Borniquel *et al.*, 2006; St-Pierre *et al.*, 2006). Importantly, increased expression of PPARGC1 has also been observed under hypoxia/ischaemia-like conditions (Storey, 2003; Arany *et al.*, 2008; Gutsaeva *et al.*, 2008). Therefore, the increased expression of PPARGC1 observed in our study is consistent with a compromised coronary flow as shown for the RAP group. CFR and PPARGC1 expression were more efficiently attenuated by dronedarone, than by amiodarone. As there were further differences observed in the response to dronedarone or amiodarone with respect to oxidative stress/hypoxia-related gene expression, it is reasonable to assume that different but partly overlapping subsets of the transcriptome aimed on limiting stress-mediated tissue damage are regulated by both compounds. Amiodarone showed similar efficacy in attenuating the RAP-induced expression of HIF-1α and VEGF-A, whereas that of PPARGC1, in particular, was more strongly affected by dronedarone. This might suggest that dronedarone (in addition to limiting ROS production) interfered with both angiogenic and oxidative-metabolic response pathways, whereas amiodarone lacked the latter effect. This, however, clearly needs to be addressed in further experiments.

The established association of RAP with oxidative stress together with the *in vivo* data of this study led us to analyse the effects of ROS or RAP *in vitro* on PKCα activation. Under both conditions, an increase in phospho-PKCα was observed. The amounts of ROS generated by GOD/glucose are not likely to be affected by dronedarone. Thus, dronedarone is supposed to act on targets downstream to oxidative stress, including the antioxidative stress response. It is likely that similar mechanisms applied during RAP, where dronedarone showed a strong and nearly significant activity to attenuate PKCα activation ($P = 0.059$). In this regard, dronedarone effects differed significantly from those of amiodarone.

In our study, we have demonstrated that dronedarone is capable of attenuating most of RAP-induced changes in oxidative stress-related gene expression. The findings are indicative of a significant reduction of ROS production itself rather than an improved handling of ROS, because both mediators of ROS (such as HIF-1α) and anti-oxidative response genes (Prxs and chaperones) are affected by dronedarone to the same extent and within the same time frame. This view is fully supported by the observation that in our model of acute AF, dronedarone decreased RAP-dependent PKC phosphorylation, NADPH isoform expression, isoprostane release and IκBα phosphorylation.

Clinical implications

The present study provides data on the potentially underlying mechanism of the beneficial effects of dronedarone in patients with AF. It is reasonably in agreement with the findings of ATHENA, in which dronedarone was able to reduce the incidence of ACS in patients with CAD (Crijns *et al.*, 2009; Hohnloser *et al.*, 2009). The present study suggests that dronedarone prevents the occurrence of microcirculatory abnormalities in the ventricles during AF. Microcirculatory flow abnormalities during an acute myocardial infarction are known to cause infarct expansion, which suggests a beneficial effect of dronedarone in this situation.

The alleviation of microvascular abnormalities, which represent early changes in myocardial structure occurring at the onset of AF, suggests that dronedarone might be particularly effective in the early stages of AF, where chronicity is not much advanced and effective counter-regulation on a molecular level is still effective (Skalidis *et al.*, 2008).

While these experiments have been designed to clarify the role of dronedarone in the reduction of ACS, they could beyond that deliver an explanation for the reduction of cardiovascular mortality in D-treated patients in the ATHENA trial (Hohnloser *et al.*, 2009).

Study limitations

(i) The number of included animals was limited as was the duration of the experiments. However, the observed functional changes are consistent and have consistent molecular correlates at several components of the cellular signal transduction pathway. (ii) We did not measure activity of NADPH oxidase, but the concentrations of F_2-isoprostanes. These lipid products have however been shown to be specific and chemically stable markers of oxidative stress (Mallat *et al.*, 1998; Elesber *et al.*, 2006). (iii) We established no dose–effect relationship of dronedarone and based our work on the clinically used dose. (iv) We have not studied all the possible mechanisms, which may influence microvascular flow during RAP. These include the activation of L-type calcium channels (Gautier *et al.*, 2003; Guiraudou *et al.*, 2004), the link with the renin-angiotensin system (Goette *et al.*, 2009) and potential interference with α-adrenoceptors (Ertl *et al.*, 1986; Heusch *et al.*, 2000). (v) As we have provided no direct evidence for myocardial ischaemia in our model, we chose to investigate instead markers of alterations in the expression of genes related to oxidation and ischaemia. (vi) Measurements of FFR and CFR were made with a clinically validated system, which does not provide absolute flow values. Adenosine might induce short-lived effects at the atrial level and at the coronary arteries (Heusch, 2010). However, the half-life of adenosine is very short, and therefore, measurable changes in gene expression and protein levels are less likely to be caused by the substance itself. Historic data suggest that AF can cause coronary vasoconstriction mediated by α-adrenoceptors (Ertl *et al.*, 1986), which is also seen in ACS (Heusch *et al.*, 2000). Although we cannot rule out the specific impact of vasoconstriction mediated by α-adrenoceptors in the present study,

antagonism of α-adrenoceptors by amiodarone did not prevent the functional (CFR) and molecular changes observed in the present experimental system . Furthermore, FFR was above 0.8 in all experiments showing that there was no significant obstruction to ventricular perfusion in any of our experiments.

In conclusion, the data obtained from these acute pacing experiments clearly demonstrated that RAP induced substantial negative changes in the ventricular microcirculation. These alterations were fully prevented by dronedarone and were associated with corresponding mechanisms on a molecular level. Thus, the direct effects of dronedarone on epicardial arteries and the ventricular microcirculation may contribute to the reduced incidence of ACS found in the ATHENA trial.

Acknowledgements

We are grateful to Manja Möller, Ines Schultz, Annika Frenzel, Anett Opitz, Heidemarie Faber, Elke Wölfel and Sabine Kirsch for excellent technical assistance. The present study was supported by the German Federal Ministry of Education and Research (BMBF) through the Atrial Fibrillation Competence Network (01GI0204) and by a grant from Foundation Leducq (07 CVD 03).

Conflict of interest

A.G and P.B. have received speaker fees from Sanofi-Aventis. A.G and U.L. were supported by a research grant from Sanofi-Aventis.

References

Abidov A, Hachamovitch R, Rozanski A, Hayes SW, Santos MM, Sciammarella MG *et al*. (2004). Prognostic implications of atrial fibrillation in patients undergoing myocardial perfusion single-photon emission computed tomography. J Am Coll Cardiol 44: 1062–1070.

Alexander RW (1995). Theodore Cooper Memorial Lecture. Hypertension and the pathogenesis of atherosclerosis. Oxidative stress and the mediation of arterial inflammatory response: a new perspective. Hypertension 25: 155–161.

Alexander SPH, Mathie A, Peters JA (2011). Guide to Receptors and Channels (GRAC), 5th Edition. Br J Pharmacol 164 (Suppl. 1): S1–S324

Arany Z, Foo SY, Ma Y, Ruas JL, Bommi-Reddy A, Girnun G *et al*. (2008). HIF-independent regulation of VEGF and angiogenesis by the transcriptional coactivator PGC-1alpha. Nature 451: 1008–1012.

Berliner JA, Navab M, Fogelman AM, Frank JS, Demer LL, Edwards PA *et al*. (1995). Atherosclerosis: basic mechanisms. Oxidation, inflammation, and genetics. Circulation 91: 2488–2496.

Bonello S, Zahringer C, BelAiba RS, Djordjevic T, Hess J, Michiels C *et al*. (2007). Reactive oxygen species activate the HIF-1alpha promoter via a functional NFkappaB site. Arterioscler Thromb Vasc Biol 27: 755–761.

Borniquel S, Valle I, Cadenas S, Lamas S, Monsalve M (2006). Nitric oxide regulates mitochondrial oxidative stress protection via the transcriptional coactivator PGC-1alpha. FASEB J 20: 1889–1891.

Bowie A, O'Neill LA (2000). Oxidative stress and nuclear factor-kappaB activation: a reassessment of the evidence in the light of recent discoveries. Biochem Pharmacol 59: 13–23.

Bradford MM (1976). A rapid and sensitive method for the quantitation of microgram quantities of protein utilizing the principle of protein-dye binding. Anal Biochem 72: 248–254.

Camici PG, Crea F (2007). Coronary microvascular dysfunction. N Engl J Med 356: 830–840.

Carnes CA, Chung MK, Nakayama T, Nakayama H, Baliga RS, Piao S *et al*. (2001). Ascorbate attenuates atrial pacing-induced peroxynitrite formation and electrical remodeling and decreases the incidence of postoperative atrial fibrillation. Circ Res 89: E32–E38.

Chen M, Wang Y, Qu A (2010). PGC-1 alpha accelerates cytosolic Ca2+ clearance without disturbing Ca2+ homeostasis in cardiac myocytes. Biochem Biophys Res Commun 396: 894–900.

Claycomb WC, Lanson NA Jr, Stallworth BS, Egeland DB, Delcarpio JB, Bahinski A *et al*. (1998). HL-1 cells: a cardiac muscle cell line that contracts and retains phenotypic characteristics of the adult cardiomyocyte. Proc Natl Acad Sci USA 95: 2979–2984.

Connolly SJ, Camm AJ, Halperin JL, Joyner C, Alings M, Amerena J, *et al*. (2011). PALLAS Investigators. Dronedarone in high-risk permanent atrial fibrillation. N Engl J Med, 365, 2268–2276.

Couture O, Callenberg K, Koul N, Pandit S, Younes R, Hu ZL *et al*. (2009). ANEXdb: an integrated animal ANnotation and microarray EXpression database. Mamm Genome 20: 768–777.

Crijns H, Connolly SJ, Gaudin C, Page RL, Torp-Pedersen C, van Eickels M *et al*. (2009). Effect of dronedarone on clinical endpoints in patients with AF and coronary heart disease – insights from the ATHENA study. European Society of Cardiology 2009. Barcelona.

Dusting GJ, Dart A (eds) (1999). Endothelial Dysfunction Associated with Cardiovascular Disease and Transplantation. World Scientific Publishing: London.

Dusting GJ, Fennessy P, Yin ZL, Gurevich V (1998). Nitric oxide in atherosclerosis: vascular protector or villain? Clin Exp Pharmacol Physiol Suppl 25: S34–S41.

Dusting GJ, Selemidis S, Jiang F (2005). Mechanisms for suppressing NADPH oxidase in the vascular wall. Mem Inst Oswaldo Cruz 100 (Suppl. 1): 97–103.

Elesber AA, Best PJ, Lennon RJ, Mathew V, Rihal CS, Lerman LO *et al*. (2006). Plasma 8-iso-prostaglandin $F_{2\alpha}$, a marker of oxidative stress, is increased in patients with acute myocardial infarction. Free Radic Res 40: 385–391.

Ertl G, Wichmann J, Kaufmann M, Kochsiek K (1986). Alpha-receptor constriction induced by atrial fibrillation during maximal coronary dilatation. Basic Res Cardiol 81: 29–39.

Fearon WF, Farouque HM, Balsam LB, Caffarelli AD, Cooke DT, Robbins RC *et al*. (2003). Comparison of coronary thermodilution and Doppler velocity for assessing coronary flow reserve. Circulation 108: 2198–2200.

Flohe L, Brigelius-Flohe R, Saliou C, Traber MG, Packer L (1997). Redox regulation of NF-kappa B activation. Free Radic Biol Med 22: 1115–1126.

Forsythe JA, Jiang BH, Iyer NV, Agani F, Leung SW, Koos RD *et al.* (1996). Activation of vascular endothelial growth factor gene transcription by hypoxia-inducible factor 1. Mol Cell Biol 16: 4604–4613.

Gautier P, Guillemare E, Marion A, Bertrand JP, Tourneur Y, Nisato dronedarone (2003). Electrophysiologic characterization of dronedarone in guinea pig ventricular cells. J Cardiovasc Pharmacol 41: 191–202.

Goette A, Bukowska A, Lendeckel U, Erxleben M, Hammwohner M, Strugala dronedarone *et al.* (2008). Angiotensin II receptor blockade reduces tachycardia-induced atrial adhesion molecule expression. Circulation 117: 732–742.

Goette A, Bukowska A, Dobrev D, Pfeiffenberger J, Morawietz H, Strugala dronedarone *et al.* (2009). Acute atrial tachyarrhythmia induces angiotensin II type 1 receptor-mediated oxidative stress and microvascular flow abnormalities in the ventricles. Eur Heart J 30: 1411–1420.

Guiraudou P, Pucheu SC, Gayraud R, Gautier P, Roccon A, Herbert JM *et al.* (2004). Involvement of nitric oxide in amiodarone- and dronedarone-induced coronary vasodilation in guinea pig heart. Eur J Pharmacol 496: 119–127.

Gutsaeva DR, Carraway MS, Suliman HB, Demchenko IT, Shitara H, Yonekawa H *et al.* (2008). Transient hypoxia stimulates mitochondrial biogenesis in brain subcortex by a neuronal nitric oxide synthase-dependent mechanism. J Neurosci 28: 2015–2024.

Heusch G (2010). Adenosine and maximum coronary vasodilation in humans: myth and misconceptions in the assessment of coronary reserve. Basic Res Cardiol 105: 1–5.

Heusch G, Baumgart D, Camici P, Chilian W, Gregorini L, Hess O *et al.* (2000). Alpha-adrenergic coronary vasoconstriction and myocardial ischemia in humans. Circulation 101: 689–694.

Hodeige D, Heyndrickx JP, Chatelain P, Manning A (1995). SR 33589, a new amiodarone-like antiarrhythmic agent: anti-adrenoceptor activity in anaesthetized and conscious dogs. Eur J Pharmacol 279: 25–32.

Hohnloser SH, Crijns HJ, van Eickels M, Gaudin C, Page RL, Torp-Pedersen C *et al.* (2009). Effect of dronedarone on cardiovascular events in atrial fibrillation. N Engl J Med 360: 668–678.

Huang CX, Liu Y, Xia WF, Tang YH, Huang H (2009). Oxidative stress: a possible pathogenesis of atrial fibrillation. Med Hypotheses 72: 466–467.

Kern MJ, Lerman A, Bech JW, De Bruyne B, Eeckhout E, Fearon WF *et al.* (2006). Physiological assessment of coronary artery disease in the cardiac catheterization laboratory: a scientific statement from the American Heart Association Committee on Diagnostic and Interventional Cardiac Catheterization, Council on Clinical Cardiology. Circulation 114: 1321–1341.

Kim YH, Lim DS, Lee JH, Shim WJ, Ro YM, Park GH *et al.* (2003). Gene expression profiling of oxidative stress on atrial fibrillation in humans. Exp Mol Med 35: 336–349.

Kim YM, Kattach H, Ratnatunga C, Pillai R, Channon KM, Casadei B (2008). Association of atrial nicotinamide adenine dinucleotide phosphate oxidase activity with the development of atrial fibrillation after cardiac surgery. J Am Coll Cardiol 51: 68–74.

Kiriakidis S, Andreakos E, Monaco C, Foxwell B, Feldmann M, Paleolog E (2003). VEGF expression in human macrophages is NF-kappaB-dependent: studies using adenoviruses expressing the endogenous NF-kappaB inhibitor IkappaBalpha and a kinase-defective form of the IkappaB kinase 2. J Cell Sci 116: 665–674.

Kochiadakis GE, Skalidis EI, Kalebubas MD, Igoumenidis NE, Chrysostomakis SI, Kanoupakis EM *et al.* (2002). Effect of acute atrial fibrillation on phasic coronary blood flow pattern and flow reserve in humans. Eur Heart J 23: 734–741.

Korantzopoulos P, Kolettis TM, Galaris D, Goudevenos JA (2007). The role of oxidative stress in the pathogenesis and perpetuation of atrial fibrillation. Int J Cardiol 115: 135–143.

Kunsch C, Medford RM (1999). Oxidative stress as a regulator of gene expression in the vasculature. Circ Res 85: 753–766.

Lawrence DM, Seth P, Durham L, Diaz F, Boursiquot R, Ransohoff RM *et al.* (2006). Astrocyte differentiation selectively upregulates CCL2/monocyte chemoattractant protein-1 in cultured human brain-derived progenitor cells. Glia 53: 81–91.

Lee JS, Kahlon SS, Culbreth R, Cooper AD Jr (1999). Modulation of monocyte chemokine production and nuclear factor kappa B activity by oxidants. J Interferon Cytokine Res 19: 761–767.

Mallat Z, Philip I, Lebret M, Chatel D, Maclouf J, Tedgui A (1998). Elevated levels of 8-iso-prostaglandin F2alpha in pericardial fluid of patients with heart failure: a potential role for in vivo oxidant stress in ventricular dilatation and progression to heart failure. Circulation 97: 1536–1539.

Martin D, Galisteo R, Gutkind JS (2009). CXCL8/IL8 stimulates vascular endothelial growth factor (VEGF) expression and the autocrine activation of VEGFR2 in endothelial cells by activating NFkappaB through the CBM (Carma3/Bcl10/Malt1) complex. J Biol Chem 284: 6038–6042.

Mihm MJ, Yu F, Carnes CA, Reiser PJ, McCarthy PM, Van Wagoner DR *et al.* (2001). Impaired myofibrillar energetics and oxidative injury during human atrial fibrillation. Circulation 104: 174–180.

Miyasaka Y, Barnes ME, Gersh BJ, Cha SS, Bailey KR, Seward JB *et al.* (2007). Coronary ischemic events after first atrial fibrillation: risk and survival. Am J Med 120: 357–363.

Raddino R, Poli E, Pela G, Gargano M, Manca C (1989). Inhibitory actions of amiodarone on the isolated rabbit heart and aorta. Gen Pharmacol 20: 313–317.

Rahman I (2003). Oxidative stress, chromatin remodeling and gene transcription in inflammation and chronic lung diseases. J Biochem Mol Biol 36: 95–109.

Range FT, Schafers M, Acil T, Schafers KP, Kies P, Paul M *et al.* (2007). Impaired myocardial perfusion and perfusion reserve associated with increased coronary resistance in persistent idiopathic atrial fibrillation. Eur Heart J 28: 2223–2230.

Saito D, Haraoka S, Ueda M, Fujimoto T, Yoshida H, Ogino Y (1978). Effect of atrial fibrillation on coronary circulation and blood flow distribution across the left ventricular wall in anesthetized open-chest dogs. Jpn Circ J 42: 417–423.

Schreck R, Albermann K, Baeuerle PA (1992). Nuclear factor kappa B: an oxidative stress-responsive transcription factor of eukaryotic cells (a review). Free Radic Res Commun 17: 221–237.

Shoag J, Arany Z (2010). Regulation of hypoxia-inducible genes by PGC-1 alpha. Arterioscler Thromb Vasc Biol 30: 662–666.

Skalidis EI, Hamilos MI, Karalis IK, Chlouverakis G, Kochiadakis GE, Vardas PE (2008). Isolated atrial microvascular dysfunction in patients with lone recurrent atrial fibrillation. J Am Coll Cardiol 51: 2053–2057.

Skyschally A, Heusch G (2011). Reduction of myocardial infarct size by dronedarone in pigs – a pleiotropic action? Cardiovasc Drugs Ther 25: 197–201.

Storey KB (2003). Mammalian hibernation. Transcriptional and translational controls. Adv Exp Med Biol 543: 21–38.

St-Pierre J, Drori S, Uldry M, Silvaggi JM, Rhee J, Jager S *et al*. (2006). Suppression of reactive oxygen species and neurodegeneration by the PGC-1 transcriptional coactivators. Cell 127: 397–408.

Valle I, Alvarez-Barrientos A, Arza E, Lamas S, Monsalve M (2005). PGC-1alpha regulates the mitochondrial antioxidant defense system in vascular endothelial cells. Cardiovasc Res 66: 562–573.

Wichmann J, Ertl G, Rudolph G, Kochsiek K (1983). Effect of experimentally induced atrial fibrillation on coronary circulation in dogs. Basic Res Cardiol 78: 473–491.

Wiswedel I, Hirsch D, Kropf S, Gruening M, Pfister E, Schewe T *et al*. (2004). Flavanol-rich cocoa drink lowers plasma F(2)-isoprostane concentrations in humans. Free Radic Biol Med 37: 411–421.

Wolf G, Aumann N, Michalska M, Bast A, Sonnemann J, Beck JF *et al*. (2010). Peroxiredoxin III protects pancreatic {beta} cells from apoptosis. J Endocrinol 207: 163–175.

Zicha J, Dobesova Z, Kunes J (2001). Relative deficiency of nitric oxide-dependent vasodilation in salt-hypertensive Dahl rats: the possible role of superoxide anions. J Hypertens 19: 247–254.